

Spontaneous domain formation in disordered copolymers as a mechanism for chromosome structuring

Matteo Negri¹, Marco Gherardi¹, Guido Tiana², and Marco Cosentino Lagomarsino³

¹Department of Physics, Università degli Studi di Milano, via Celoria 16, 20133 Milano, Italy

²Center for Complexity and Biosystems and Department of Physics, Università degli Studi di Milano and INFN, via Celoria 16, 20133 Milano, Italy

³Sorbonne Universités, UPMC Univ Paris 06, UMR 7238, Computational and Quantitative Biology, 4 Place Jussieu, Paris, France; CNRS, UMR 7238, Paris, France; IFOM, Milan, Italy

August 10, 2021

Abstract

Motivated by the problem of domain formation in chromosomes, we studied a co-polymer model where only a subset of the monomers feel attractive interactions. These monomers are displaced randomly from a regularly-spaced pattern, thus introducing some quenched disorder in the system. Previous work has shown that in the case of regularly-spaced interacting monomers this chain can fold into structures characterized by multiple distinct domains of consecutive segments. In each domain, attractive interactions are balanced by the entropy cost of forming loops. We show by advanced replica-exchange simulations that adding disorder in the position of the interacting monomers further stabilizes these domains. The model suggests that the partitioning of the chain into well-defined domains of consecutive monomers is a spontaneous property of heteropolymers. In the case of chromosomes, evolution could have acted on the spacing of interacting monomers to modulate in a simple way the underlying domains for functional reasons.

1 Introduction

Simple heteropolymer models provide a candidate explanation for the formation of intermediate- and large-scale domains in prokaryotic and eukaryotic chromatin [1, 2, 3, 4, 5]. Such domains may be defined as extended contiguous regions along the DNA chain in which the DNA interacts preferentially with sites of the same domain. As such, they appear as squared blocks in the contact matrix of the polymer, which is measurable by chromosome capture and sequencing techniques [3]. While other mechanisms, such as loop extrusion [6, 7] likely contribute to driving domain formation, the interaction between chromosome-bound proteins is considered to be one of the main drivers for this behavior. For example, in mammals, the protein CTCF has been shown to form dimers [8] that can stabilize chromatin loops. In bacteria, the proteins H-NS and MatP have the same bridging capabilities [4, 9]. One main question is what drives domain identity, size and stability, and to what extent intra-specific interactions are needed to form domains. In other words, while it is rea-

sonable to think that the domain formation is mediated by proteins that are bound to chromatin and that interact with each other, we do not know how many species are needed to program a certain number of domains into a polymer [3]. Since there are thousands of domains at different scales in mammalian genomes, trivially associating one-to-one interactions would require the presence of thousands of different types of intra-specific DNA-binding proteins. It is more reasonable to think that only a small number of proteins is responsible for the interactions between the chromatin sites.

Focusing on the direct interaction between chromatin structure factors, various kinds of heteropolymer models [3, 10, 11, 12] have been proposed, to explain various aspects of domain formation, specification and stability. Perhaps the simplest one is a polymer chain in which equally-spaced monomers attract monomers of the same type [12, 13]. This is a specific type of co-polymer model in which only one of the two chemical species exerts attractive interactions (and the linear density of this species is typically considered to be low). This model shows that multiple-domain states are possible without any intra-specific interaction [13]. In such states, the polymer is collapsed into a multiple rosette configuration. Analytical arguments support the hypothesis that such multi-domain phase is stable, and due to the trade-off between the surface-tension cost of keeping a core of bridging proteins and the entropy cost of the arms of the rosette states.

Here, we use replica-exchange Monte Carlo (MC) simulations to explore the equilibrium states of the disordered version of this model, where the interacting monomers are not equally spaced, but arranged randomly along the backbone in a fixed (quenched) configuration. We ask about the role played by these disordered interactions into the thermodynamic stability of the collapsed states with one and multiple domains. We also address the possible role of the disorder into localizing the domains in a specific region of the chain, which may lead to pre-programmed spatial domains without intra-specific interactions.

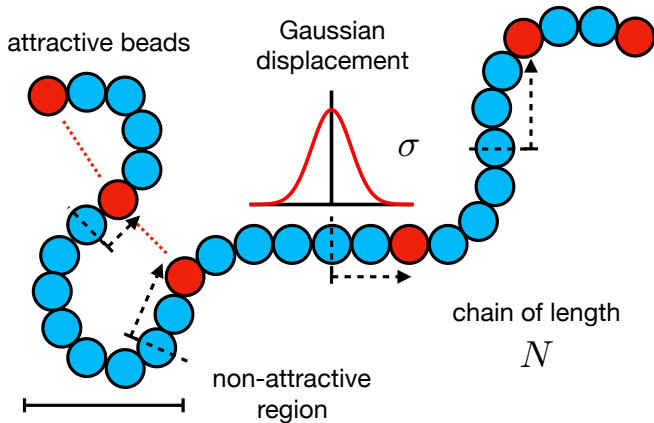


Fig. 1: Sketch of the model used in this work. The polymer is made of two types of monomers. Short-ranged attractive monomers (red) are separated by regions of non-attractive ones (light-blue). The position of attractive monomers is fixed at distance extracted from a Gaussian distribution, and attractive monomers are fixed during each simulation (quenched disorder). Monomers are described as hard-sphere beads, joint by inextensible links.

2 Model

We study a coarse-grained model consisting in a polymer made of N consecutive monomers represented as hard-sphere beads of radius R_{HC} (see Fig.1). Each monomer represents a region of the chromosome, and the size can be defined at will to describe the fiber at any resolution (e.g., from the finest experimental resolution of \sim kb to describe topological associating domains, to that of Mb to describe chromosomal compartments). In this model, bead i can interact with bead j with an attractive short-ranged square well potential u_{ij} :

$$u_{ij} = \begin{cases} \infty & \text{if } r_{ij} < R_{\text{HC}} \\ B_{ij} & \text{if } R_{\text{HC}} < r_{ij} < R \\ 0 & \text{if } r_{ij} > R, \end{cases}$$

where r_{ij} is the distance between the beads, R_{HC} is the hard-core radius, R is the range of the interaction and B_{ij} is the interaction energy, which depends on the types of the monomers i and j . In order to represent bridging interactions, we place p attractive monomers along the chain (see Fig.1). Therefore, the interaction energy is

$$B_{ij} = \begin{cases} -\varepsilon & \text{if } i \text{ and } j \text{ are attractive monomers} \\ 0 & \text{otherwise} \end{cases}$$

where $\varepsilon > 0$ since the interaction between bridging points is always attractive.

Using square-well potentials makes the MC calculations easier and faster than using smooth short-ranged potential. The uncrossability of the polymer chain is guaranteed by the hard-core repulsion, whose range is $R_{\text{HC}} = 0.472\lambda$. The distance λ between consecutive beads is maintained fixed by the MC moves, and sets the microscopic length scale, with respect to which all the lengths of the model are measured.

We first studied regular co-polymers, in which interacting monomers are placed every p other monomers which

only repel each other by hard-core repulsion. Subsequently, we studied a disordered model in which the position of these interacting monomers is displaced by a Gaussian-distributed quantity.

The simulations are performed with an off-lattice MC algorithm whose degrees of freedom are the angles and dihedrals of the chain, updated with flip and pivot moves through a Metropolis acceptance rule, to ensure an effective sampling of the canonical ensemble. The algorithm is implemented in a freely-distributed code [14]. To improve the efficiency of the algorithm to sample equilibrium conformations also at low temperatures, the MC algorithm is used in its parallel-tempering variant, in which 16 replicas of the system are simulated in parallel at increasing temperature, and the conformations of adjacent temperatures are exchanged every 1000 MC step with a Metropolis-like acceptance rule [15]. The thermodynamic quantities are then calculated with a weighted-histogram technique [16].

3 Results

Multi-domain states in absence of disorder are stable

In the case of equally-spaced bridging points, theoretical arguments support the claim that multi-domain states are thermodynamically stable [13]. To test this hypothesis, we simulated polymers from $N = 129$ up to $N = 513$ monomers with the parallel-tempering algorithm until the quantities of interest reached convergence, keeping constant the density of interacting monomers $\eta = p/N$. As shown in Fig. 2, polymers with $N = 129$ monomers collapse into a single domain, while the polymers of length $N = 256$ and $N = 513$ collapse into a multiple-domain state similar to rosettes. Rosettes are formed by consecutive strands of the chain. In this range of N , the number of domains seems to depend linearly on p , as suggested in ref. [13]. The collapse for all values on N happens near a temperature of $T \simeq 0.47\varepsilon$ (see Fig. 2). No phase similar to a random globule, in which the interactions are not correlated with the distance of the interacting monomers along the chain, is observed. All the rosette-like and multiple-rosette configurations appear to be thermodynamically stable below the coil-globule transition temperature (see Supplementary Figure S1).

For longer chains ($N > 129$), after a first collapse at higher temperature, the polymer displays a second collapse at lower temperature from a phase with higher number of domains to a phase with a lower number of domains (e.g., see Fig. 2, red solid curve). While the first energy jump displays features similar to a first-order phase transition, as suggested in [13], the fusion of two domains resembles a nucleation-like phenomenon, and we speculate that this could be similar to a second order phase transition. The low-temperature phases are difficult to sample for longer polymers and thus we could not equilibrate the chain with $N = 513$ below $T = 0.14\varepsilon$. Although we have seen in this range of low temperatures conformations with three and two rosettes, we are not able to assess if they are equilibrium states. Equally, we could not equilibrate the system at even lower temperatures, at which we expect the equilibrium state to form a single rosette, because this

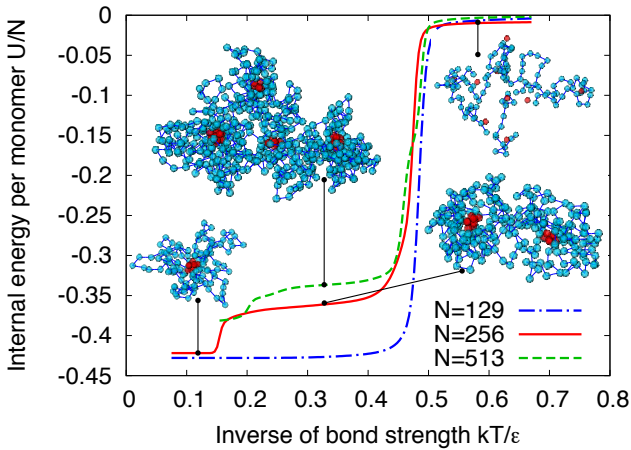


Fig. 2: Energy density for co-polymers with an ordered pattern of interacting monomers. In these simulations the density of interacting monomers $\eta = p/N$ was kept constant to the value $1/16$. Simulations were performed with $\varepsilon = 2.4$, $R = 0.77$, $\lambda = 1.42$ for 3×10^9 Monte Carlo sweeps.

is certainly the zero-temperature equilibrium state of the system.

Summing up, our results indicate that new stable multi-domain phases become available with increasing system size, and that the system can cross several hierarchical levels of organization with decreasing number of domains as equilibrium states as the temperature is decreased, before collapsing into a single domain.

Disorder enhances the stability of multi-domain configurations

The model with interacting monomers placed every η^{-1} other monomers is then extended, introducing a quenched Gaussian displacement of zero mean and variance σ . For $\sigma = 0$ we recover the ordered case, while for $\sigma \gtrsim \eta^{-1}$ we expect a uniform distribution of interacting monomers, not reminiscent of the ordered arrangement.

Before studying the equilibrium properties of the disordered system, we must show that they are self-averaging, that is that the average over the disorder is representative of a typical situation. As a rule, extensive quantities like the internal energy are self-averaging because of an argument given by Brout [17]; however this argument cannot be applied straightforwardly to disordered polymers, and we checked explicitly in two cases ($\sigma = 7$ and $\sigma = 16$, using four realizations of the disorder) that the energy curves and the number of rosettes do not depend on the specific realization of the disorder (see Fig. S2 in the Supplementary Material).

We then performed equilibrium simulations with $\eta^{-1} = 16$ and σ varying from 0 to 32 for $N = 257$. In all these cases, as shown in Fig. 3, we observe a transition from a random coil at high temperatures to multi-rosette states. The transition becomes less sharp with increasing σ . Moreover, the disorder has the unexpected effect of stabilizing the multi-domain phase, as the transition temperatures become higher. This effect is accompanied by a broadening of the range of temperatures in which

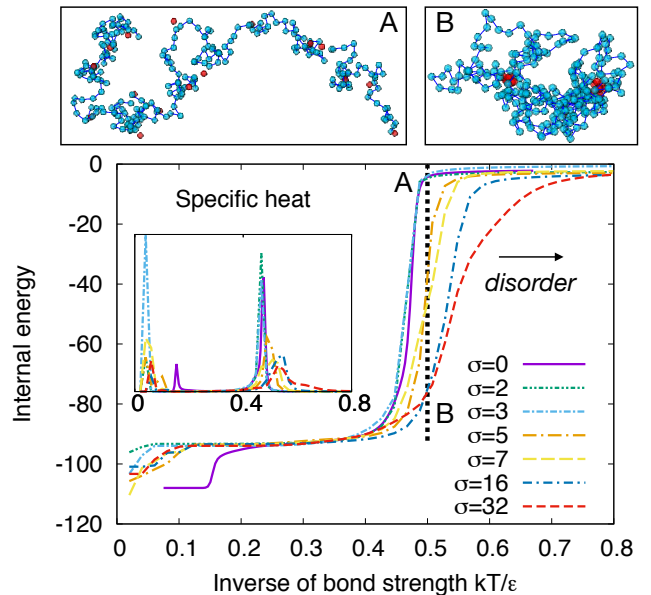


Fig. 3: Disorder in the positioning of the interacting monomers shifts the domain-formation transition towards higher temperatures. The plot shows collapse curves of internal energy of a polymer of length $N = 257$ monomers. Each dashed curve relates to a different value of the variance σ . Two snapshots at the same temperature are highlighted comparing the case of regularly-spaced interacting monomers (A) to the disordered case (B): while the former is clearly in a coil state, the latter appears collapsed into a two-domain state. This is also visible in the specific heat vs kT/ε plot (inset), in which the peak corresponding to the transition point smoothens and shifts towards higher temperatures in presence of disorder. The simulations were performed with $N = 257$, $\eta = 17/257$, $R = 0.77$, $\lambda = 1.42$, $1.8 \cdot 10^9$ MC moves.

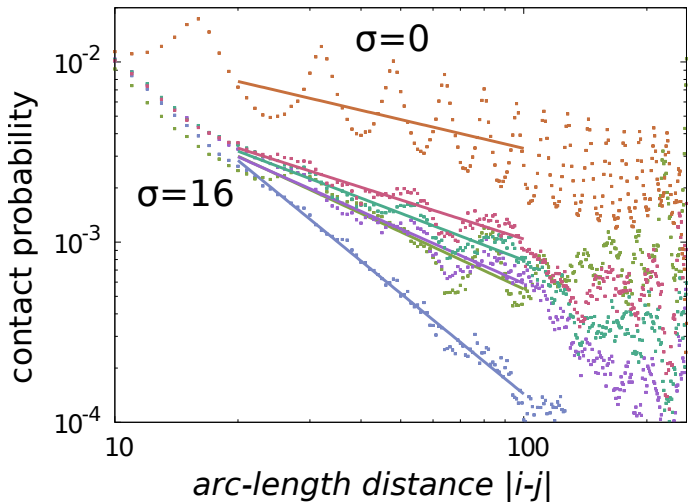


Fig. 4: The model shows power-law like scaling of the contact probability with arc-length distance. The plot shows the mean logarithm of the contact probability obtained from simulations. The average is performed over configurations and over all monomers i and j , whose intermonomer distance is $|i - j|$. The different curves correspond to the case of ordered interacting monomers ($\sigma = 0$, orange points) and disordered interacting monomers, $\sigma = 16$ at temperatures $T = 0.49$ (red), $T = 0.50$ (cyan), $T = 0.52$ (green and purple, for two different realizations of the disorder), $T = 0.53$ (blue). The solid lines are linear fits, giving slopes (exponents) 0.53 for $\sigma = 0$, 0.72 for $\sigma = 16$ at $T = 0.49$, 0.87 at $T = 0.50$, 1.01 and 1.05 at $T = 0.52$ and 1.86 at $T = 0.53$.

the multiple domain phase is stable, roughly proportional to σ . The inset of Fig. 3 shows the specific heat of the system, whose peaks are associated with the transitions. Two peaks in the specific heat are typically visible in this plot, corresponding, respectively, to the collapse from coil to two-domain state (high temperature) and to the transition from two-domain state to one-domain state (low temperature). These peaks shift apart at increasing σ . The disorder smoothens the collapse curve of the higher transition only, since the height of the specific-heat peak decreases with σ , while it becomes wider. This suggests that the transition from coil to multiple-domain states may no longer be switch-like, due to the emergence of domains of different size at different temperatures.

We also considered the average contact probability between monomers as a function of their distance $|i - j|$ along the chain, which is typically measured from genome contact maps [1, 3]. Fig. 4 compares this function for the case of equally-spaced and disordered interacting monomers. In the ordered case ($\sigma = 0$), the spacing with the closest interacting induces oscillations in the function, but the overall trend agrees with a power law with exponent close to 0.5 for values of $|i - j|$ up to distances comparable to N (and therefore affected by finite-size effects). Disordered chains display exponents that increase with the temperature between, 0.7 and 1 in the multi-rosette phase, and up to 1.9 in the coil region (this value is comparable to the expectation for a self-avoiding chain). The exponents appear to depend weakly on the specific realization of the disorder (cf. purple and green points in Fig. 4).

Scaling argument for the entropy of a disordered star polymer

In order to give some theoretical support to explain why the multi-rosette configurations are thermodynamically stable in presence of disorder, we generalized the scaling argument given in ref. [13]. In a configuration made of q rosettes, each domain has a core made of p/q monomers and a corona made of p/q loops. Each rosette is approximated as a star polymer made of $f = p/q$ arms. This description allows a simple estimate of the entropic contribution of the corona to the free energy. In absence of disorder the leading term in this contribution is $f^{3/2}$. The energetic contribution to the free energy is the surface tension of each core, which is proportional to the surface of a single core $(p/q)^{2/3}$ multiplied by the number of domains. Therefore, the free energy in absence of disorder reads

$$\Delta F \simeq p^{3/2} q^{-1/2} + \varepsilon(p)^{2/3} q^{1/3}, \quad (1)$$

which can be minimized with respect to the number of domains q , to find the number of rosettes at equilibrium

$$q_{\text{eq}} \sim \varepsilon^{-6/5}. \quad (2)$$

We now estimate how ΔF changes for disordered distributions of bridging points in the polymer. At fixed rosette state, the changes in the positions of the attractive monomers along the chain do not affect the energetic term, so we need to compute only the entropic term for a rosette with loops of random length. To do this, we approximate the disordered rosette to a star polymer with arms of random length, and use the blob model for star polymers [18, 19] to describe the system with a mean-field ansatz. Here we omit intermediate calculations, which can be found in the supplementary material, section S1. To account for the different lengths of the arms, we impose that the number of arms f is a decreasing function of the radius,

$$f(r) = f_0 \left(\frac{r}{b}\right)^{-\gamma}, \quad (3)$$

where b is the radius of the core of the star and $\gamma \geq 0$. It is possible to show that this is equivalent to a power-law distribution of the distance between consecutive attractive monomers (see supplementary material, section S1, last paragraph). This assumption does not correspond to the Gaussian displacements of the bridging points from equally-spaced positions used in our simulations, and is motivated mainly by the ease of carrying out the calculation.

We can now plug Eq. 3 into a scaling argument similar to the one found in ref. [19]. This calculation gives a leading term in the entropy that is identical to the one in absence of disorder,

$$\Delta F_{\text{entropic}} \simeq f_0 \left[S - \gamma f_0^{-1/2} \frac{S^2}{2} + \frac{\gamma^2}{4} f_0^{-1} \frac{S^3}{3} \right] \quad (4)$$

with

$$S \simeq \frac{2}{\gamma} f_0^{1/2},$$

which implies

$$\Delta F_{\text{entropic}} \simeq (f_0)^{3/2}. \quad (5)$$

Thus, this argument supports the existence of stable states in presence of disorder in the bridging points, and predicts

that the disorder does not change the leading term in the entropy of the rosettes, and the collapse is qualitatively the same. Since the leading-order term of the entropy is unaffected in the extreme power-law spacing between attracting monomers along the chain, we also expect that this prediction applies for more compact distributions of the spacing between possible bridging points, such as the one used in our simulations. Indeed, we find that the collapsed phase of the polymer of length $N = 257$ exhibits two domains for all values of σ we tested, just as the model in absence of disorder.

In order to rationalize why the simulations show a shift of the transition towards higher temperatures, which is not predicted by the above argument, we can notice that the above argument only considers the star-polymer contribution to the free energy. We can also compare the typical value of the loop entropy in presence and absence of disorder, but at fixed η . In absence of disorder the total entropy of p loops of length N/p is

$$S_{\text{tot}} \sim p \log(N/p). \quad (6)$$

For sufficiently small disorder (i.e. when σ is much smaller than η^{-1}), there are p loops of random length $l_i = |x_i - x_{i+1}|$, where x_i and x_{i+1} are the positions of two consecutive attractive monomers. Since the distribution of x_i is Gaussian, the distribution of l_i is still a Gaussian with mean $\langle l_i \rangle = N/p$. Thus we can compute the total entropy for the system in presence of disorder:

$$S_{\text{tot}}^{\text{dis}} \sim \sum_{i=1}^p \log(l_i). \quad (7)$$

We can rewrite eq. 7 to obtain a relation with S_{tot} :

$$\begin{aligned} S_{\text{tot}}^{\text{dis}} &\simeq p \sum_{i=1}^p \frac{1}{p} \log(l_i) \\ &\simeq p \langle \log(l_i) \rangle < p \log \langle l_i \rangle \end{aligned}$$

where in the last line we used the Jensen inequality for concave functions. This means that

$$S_{\text{tot}}^{\text{dis}} < S_{\text{tot}},$$

namely that the entropy cost for p loops decreases in the disordered model, so that the transition temperature increases. For the same reason, allowing for collapsed states with multiple domains, one can also speculate that the transition becomes broader because different regions of the polymer with different local densities of attractive monomers start to collapse at different temperatures.

Localization of domains caused by disorder

In long ordered co-polymers with equally-spaced attracting monomers, the positions of the domains are invariant for translations along the chain, and they are free to move along the chain (see Fig. 5, left column). Different equilibrium conformations can break this symmetry, displaying domains at specific positions, but the equilibrium contact map averages out the domains, re-establishing the translational symmetry (cf. the lowest-left contact map in Fig. 5). Only a small effect due to the finiteness of the chain is observable at the polymer ends; this would further reduce in longer, more realistic polymers.

Disorder has the effect of localizing the domains, preventing their averaging out. The three rightmost columns of Fig. 5 show the result of simulations performed with a realization of disorder with $\sigma = 3$ and two realizations with $\sigma = 16$, choosing $N = 257$ and $p = 17$. Disorder breaks the translational symmetry of the system, favouring the stabilization of domains in specific regions of the chain. As a consequence, the average map is no longer uniform. For example, at $\sigma = 3$, contact maps show with high probability a two-blocks structure (figure 5, second column, bottom panel) that highly contribute to determine the average map (shown below).

As shown in the case $\sigma = 16$ (last two columns of Fig. 5), the degree of localization depends on the specific realization of the disorder. The figure shows two contact maps of conformations obtained with two different realizations of the same distribution of disorder. In the first realization, the two-block structure has well-defined borders that correspond the regions around monomer 25 and 110. Instead, the second realization of the same distribution does not show a clear compartmentalization into two fixed spatial domains, and reallocation of bridging points is observed around a coarse-grained nearly equally-spaced structure of organizing centers. The degree of localization of the domains does not seem to depend trivially on the organization of the interacting monomers into linear clusters along the chain (green dots along the diagonal of Fig. 5). In the case $\sigma = 3$, the displacement from the ordered case is small, but still there is a higher degree of localization than the case $\sigma = 16$ shown in the rightmost column, where there is a more marked partitioning of interacting monomers. Thus, the degree of localization appears to result from a complex balancing between energy and entropy, and cannot be easily predicted from the location of the interacting monomers.

4 Discussion and Conclusions

Our extensive MC simulations give access to the equilibrium properties of polymers up to up to $N = 513$, characterized by a small linear density of fixed attractive monomers, which can be equally spaced or disordered. Both in the ordered and disordered case, the phase diagram of the polymer displays a high-temperature coil phase and a sharp transition to globular phases with multi-rosette structures. The states with different number of rosettes are clearly separated from each other by jumps in the internal energy which resemble first-order transitions. At highest temperatures we observe states with the largest number of rosettes, and this number decreases with the temperature to the one-rosette zero-temperature state. Although the system size is limited in our simulations by the high computational cost of equilibrating the system, we can speculate that a hierarchy of states exists with varying number of rosettes. The maximum observed number, $n_{\text{max}} \simeq N/128$, is reached just below the coil-globule transition temperature. The observed rosettes have the specific feature of involving monomers that are close along the chain.

The formation of rosette-like domains is a form of microphase separation (MPS), which the thermodynamic limit is known to take place in ordered co-polymers and to

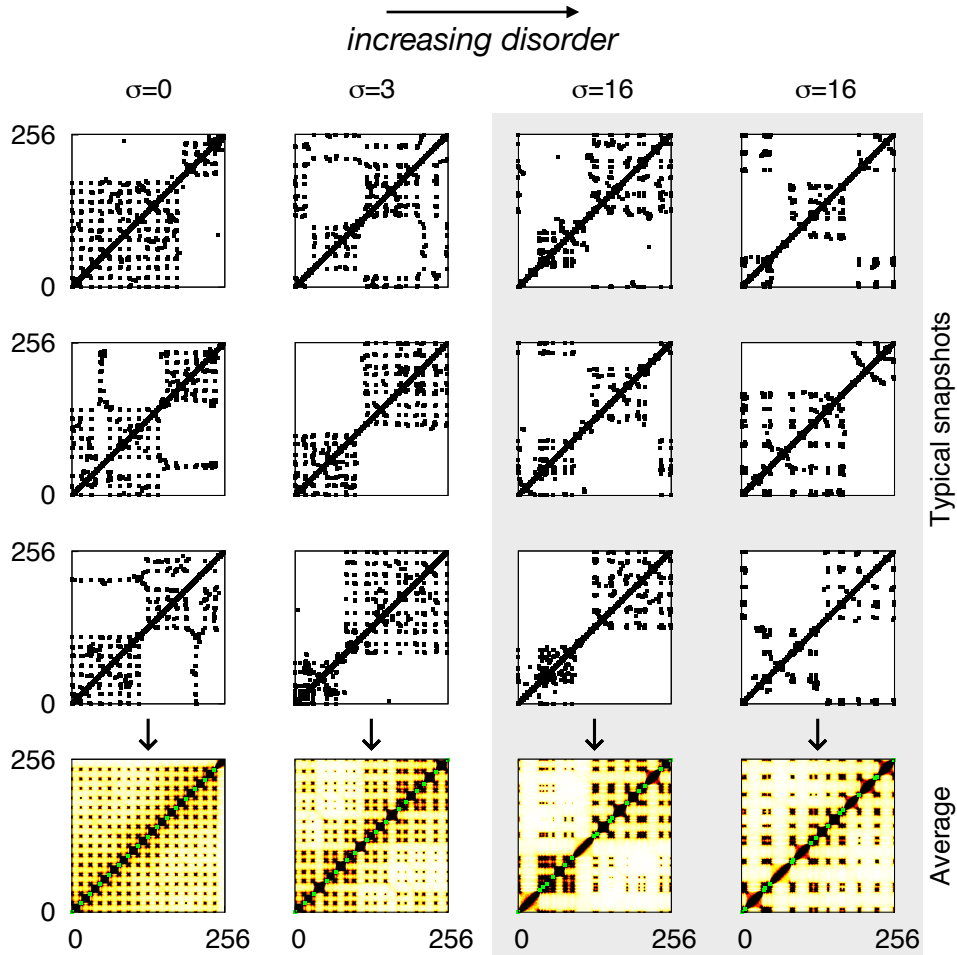


Fig. 5: A disordered distribution of interactions can localize the domains along the chain. The figure shows contact matrices for different conformations of a polymer made of $N = 257$ monomers and $p = 17$ interacting monomers (in green) distant 16 monomers from each other. The lowest contact maps are the equilibrium average of the system. Each column is obtained with a specific realization of the disorder, while the two columns with $\sigma = 16$ are obtained, respectively, with two different realizations of the placement of interacting beads. These simulations were performed with $N = 257$, $\eta = 17/257$, $R = 0.77$, $\lambda = 1.42$, $1.8 \cdot 10^9$ Monte Carlo sweeps. The replicas used in this image are at the temperature $k_B T / \varepsilon = 0.3$.

produce well-defined structures with few allowed symmetries (lamellar, hexagonal and cubic) in the vicinity of the homogeneous phase [20]. If disorder is added in the position of the chemical species, mean-field calculations by de Gennes show that the MPS phase is suppressed in favour of a glassy state [21]. Beyond mean field, Shakhnovich and coworkers showed that fluctuations reduce the glassy temperature re-establishing the MPS [22], by a perturbative approach in the number of neighbouring monomers common to different conformations of the chain (disregarded in the mean field). Our results suggest that correlations between neighbouring monomers play an important role in defining the phase diagram of this polymer. Although the size of our polymers is limited by computational constraints, the rosette-like domains we observed are formed by consecutive segments of the chain, and suggest that effect of correlations could be much larger than that suggested by the perturbative approach. In fact, while the latter predicts a phase diagram with a second-order transition from a disordered globule to MPS, we observe what looks like a first-order transition from a random coil directly to a domain-separated phase. Moreover, at increasing disorder, the range of temperatures at which MPS occurs increases not only because the freezing temperature decrease, as predicted in ref. [22], but also because the high-energy states are affected (as observed in ref. [23]), increasing the coil-globule transition temperature.

Whether this behaviour is a result of the finiteness of the chain or is a feature that survives in the thermodynamic limit, we cannot tell based on our simulations, which are necessarily limited in terms of the size of the chain. However, the scaling arguments that support the simulations are not expected to fail in the large- N limit, suggesting that the phase diagram we propose is stable with respect to N .

An important effect of the disorder is that of localizing the structural domains in the chain, analogously to what happens with spin diffusion in the presence of impurities [24]. While the system, at least in the thermodynamic limit, is invariant for translation of the domains, and consequently its average equilibrium contact map is uniform, in presence of quenched disorder the domains can become localized, resulting in a block equilibrium contact map. The detailed pattern of blocks, and even how well-defined they are, does not appear to be a self-averaging quantity, and depends on the specific positioning of the interacting monomers. These properties do not seem to be easily predicted from the knowledge of the exact realization of disorder, in agreement with the general observation that the identification of the equilibrium states of disordered systems is a NP-hard problem [25].

The results obtained with this simple co-polymer model can be useful to get some insight in the structural organization of chromosomes [26], which display a hierarchical set of nested domains [27]. Little is known about the actual molecular mechanisms responsible for the formation of domains, at different length scales, in the chromatin fiber and several models were proposed to account for such an organization. Some years ago it was suggested that they are the result of the rapid collapse of the fiber into a non-equilibrium crumpled globule [28]. A model that generates blocks that are similar to the smallest-scale domains observed in chromatin is the loop-extrusion, based

on the hypothesis that the interaction between regions of the fiber are mediated by an active, ATP-fueled protein complex [6, 7]. In other, equilibrium, models, such as the one we study here, the number of domains is determined by the number of different interacting species [29, 30], and the formation of domains is essentially energy-driven. With the present simple model we showed that it is not necessary to resort to very complicated ingredients, but the balance between entropy and energy is enough to generate stable domains even with a single type of interacting protein.

Finally, a feature of chromosomes that emerges from experimental data and that was widely studied in the past years is that the contact probability between pairs of regions of the same chromosome roughly scales with their genomic distance with a power law controlled by an atypical exponent that is variable, but typically lower than 1.5, behavior that is unexpected for simple homopolymers at equilibrium [31, 32]. Also in this case several physical mechanisms were proposed [31, 33, 34, 6]. Our results suggest that even a simple model as the one we propose here produces equilibrium contact probability functions that can be fitted with power laws of genomic distance, with exponents that are lower than those of homopolymers, and in overall agreement with the trends of experimental data. In our model, the slopes of this contact probability depend on the disorder strength and on the stabilization energy of the domains.

References

- [1] M. V. Imakaev, G. Fudenberg, and L. A. Mirny, "Modeling chromosomes: Beyond pretty pictures," *FEBS letters*, vol. 589, no. 20PartA, pp. 3031–3036, 2015.
- [2] M. Cosentino Lagomarsino, O. Espéli, and I. Junier, "From structure to function of bacterial chromosomes: Evolutionary perspectives and ideas for new experiments.," *FEBS Lett*, vol. 589, pp. 2996–3004, Oct 2015.
- [3] M. Nicodemi and A. Pombo, "Models of chromosome structure," *Current opinion in cell biology*, vol. 28, pp. 90–95, 2014.
- [4] R. T. Dame, O. J. Kalmykova, and D. C. Grainger, "Chromosomal macrodomains and associated proteins: implications for dna organization and replication in gram negative bacteria.," *PLoS Genet*, vol. 7, p. e1002123, Jun 2011.
- [5] W. Schwarzer, N. Abdennur, A. Goloborodko, A. Pekowska, G. Fudenberg, Y. Loe-Mie, N. A. Fonseca, W. Huber, C. H. Haering, L. Mirny, *et al.*, "Two independent modes of chromatin organization revealed by cohesin removal," *Nature*, vol. 551, no. 7678, p. 51, 2017.
- [6] G. Fudenberg, M. Imakaev, C. Lu, A. Goloborodko, N. Abdennur, and L. A. Mirny, "Formation of chromosomal domains by loop extrusion," *Cell reports*, vol. 15, no. 9, pp. 2038–2049, 2016.

- [7] A. Goloborodko, J. F. Marko, and L. A. Mirny, “Chromosome compaction by active loop extrusion,” *Biophysical journal*, vol. 110, no. 10, pp. 2162–2168, 2016.
- [8] V. Pant, S. Kurukuti, E. Pugacheva, S. Shamsuddin, P. Mariano, R. Renkawitz, E. Klenova, V. Lobanenkova, and R. Ohlsson, “Mutation of a single ctfc target site within the h19 imprinting control region leads to loss of igf2 imprinting and complex patterns of de novo methylation upon maternal inheritance,” *Molecular and cellular biology*, vol. 24, no. 8, pp. 3497–3504, 2004.
- [9] M. C. Noom, W. W. Navarre, T. Oshima, G. J. Wuite, and R. T. Dame, “H-ns promotes looped domain formation in the bacterial chromosome,” *Curr Biol*, vol. 17, no. 21, pp. R913–4, 2007.
- [10] C. A. Brackley, J. Johnson, S. Kelly, P. R. Cook, and D. Marenduzzo, “Simulated binding of transcription factors to active and inactive regions folds human chromosomes into loops, rosettes and topological domains,” *Nucleic acids research*, vol. 44, no. 8, pp. 3503–3512, 2016.
- [11] L. I. Nazarov, M. V. Tamm, V. A. Avetisov, and S. K. Nechaev, “A statistical model of intra-chromosome contact maps,” *Soft Matter*, vol. 11, no. 5, pp. 1019–1025, 2015.
- [12] I. Junier, O. Martin, and F. Képès, “Spatial and topological organization of dna chains induced by gene co-localization,” *PLoS computational biology*, vol. 6, no. 2, p. e1000678, 2010.
- [13] V. F. Scolari and M. C. Lagomarsino, “Combined collapse by bridging and self-adhesion in a prototypical polymer model inspired by the bacterial nucleoid,” *Soft matter*, vol. 11, no. 9, pp. 1677–1687, 2015.
- [14] G. Tiana, F. Villa, Y. Zhan, R. Capelli, C. Paissoni, P. Sormanni, E. Heard, L. Giorgetti, and R. Meloni, “Montegrappa: an iterative monte carlo program to optimize biomolecular potentials in simplified models,” *Computer Physics Communications*, vol. 186, pp. 93–104, 2015.
- [15] R. H. Swendsen and J.-S. Wang, “Replica monte carlo simulation of spin-glasses,” *Physical Review Letters*, vol. 57, no. 21, p. 2607, 1986.
- [16] A. M. Ferrenberg and R. H. Swendsen, “Optimized monte carlo data analysis,” *Physical Review Letters*, vol. 63, no. 12, p. 1195, 1989.
- [17] R. Brout, “Phys. Rev. 115, 824 (1959) - Statistical Mechanical Theory of a Random Ferromagnetic System,” *Physical Review*, 1959.
- [18] M. Daoud and J. Cotton, “Star shaped polymers: a model for the conformation and its concentration dependence,” *Journal de Physique*, vol. 43, no. 3, pp. 531–538, 1982.
- [19] T. Witten and P. Pincus, “Colloid stabilization by long grafted polymers,” *Macromolecules*, vol. 19, no. 10, pp. 2509–2513, 1986.
- [20] L. Leibler, “Theory of Microphase Separation in Block Copolymers,” *Macromolecules*, vol. 13, pp. 1602–1617, Nov. 1980.
- [21] P. G. de Gennes, “Theory of long-range correlations in polymer melts,” *Faraday Discussions of the Chemical Society*, vol. 68, pp. 96–103, Jan. 1979.
- [22] C. D. Sfatos, A. M. Gutin, and E. I. Shakhnovich, “Phase diagram of random copolymers,” vol. 48, no. 1, pp. 465–475, 1993.
- [23] G. Tiana and L. Sutto, “Equilibrium properties of realistic random heteropolymers and their relevance for globular and naturally unfolded proteins,” vol. 84, p. 061910, Dec. 2011.
- [24] P. W. Anderson, “Absence of Diffusion in Certain Random Lattices,” *Phys. Rev.*, vol. 109, pp. 1492–1505, 1958.
- [25] F. Barahona, “On the computational complexity of Ising spin glass models,” *Journal of Physics A: Mathematical and General*, vol. 15, pp. 3241–3253, Oct. 1982.
- [26] L. Ringrose, *Epigenetics and Systems Biology*. Academic Press, 2017.
- [27] Y. Zhan, L. Mariani, I. Barozzi, E. G. Schulz, N. Blüthgen, M. Stadler, G. Tiana, and L. Giorgetti, “Reciprocal insulation analysis of Hi-C data shows that TADs represent a functionally but not structurally privileged scale in the hierarchical folding of chromosomes,” *Genome Research*, vol. 27, pp. 479–490, Mar. 2017.
- [28] L. A. Mirny, “The fractal globule as a model of chromatin architecture in the cell,” *Chromosome research*, vol. 19, no. 1, pp. 37–51, 2011.
- [29] D. Jost, P. Carrivain, G. Cavalli, and C. Vaillant, “Modeling epigenome folding: formation and dynamics of topologically associated chromatin domains,” *Nucleic Acids Research*, vol. 42, pp. 9553–9561, Sept. 2014.
- [30] S. Bianco, A. M. Chiariello, C. Annunziatella, A. Esposito, and M. Nicodemi, “Predicting chromatin architecture from models of polymer physics,” *Chromosome research : an international journal on the molecular, supramolecular and evolutionary aspects of chromosome biology*, vol. 25, pp. 25–34, Mar. 2017.
- [31] E. Lieberman-Aiden, N. L. van Berkum, L. Williams, M. Imakaev, T. Ragozy, A. Telling, I. Amit, B. R. Lajoie, P. J. Sabo, M. O. Dorschner, R. Sandstrom, B. Bernstein, M. A. Bender, M. Groudine, A. Gnirke, J. Stamatoyannopoulos, L. A. Mirny, E. S. Lander, and J. Dekker, “Comprehensive mapping of long-range interactions reveals folding principles of the human genome,” *Science*, vol. 326, pp. 289–293, Oct. 2009.
- [32] A. L. Sanborn, S. S. P. Rao, S.-C. Huang, N. C. Durand, M. H. Huntley, A. I. Jewett, I. D. Bochkov, D. Chinnappan, A. Cutkosky, J. Li, K. P. Geeting,

- A. Gnirke, A. Melnikov, D. McKenna, E. K. Stamenova, E. S. Lander, and E. L. Aiden, “Chromatin extrusion explains key features of loop and domain formation in wild-type and engineered genomes,” *Proceedings of the National Academy of Sciences of the United States of America*, vol. 112, pp. E6456–E6465, Nov. 2015.
- [33] M. Barbieri, M. Chotalia, J. Fraser, L.-M. Lavitas, J. Dostie, A. Pombo, and M. Nicodemi, “Complexity of chromatin folding is captured by the strings and binders switch model,” *Proceedings of the National Academy of Sciences of the United States of America*, vol. 109, pp. 16173–16178, Oct. 2012.
- [34] Y. Zhan, L. Giorgetti, and G. Tiana, “Looping probability of random heteropolymers helps to understand the scaling properties of biopolymers,” vol. 94, pp. 032402–10, Sept. 2016.